Improved radiosynthesis and preliminary in vivo evaluation of the ^{11}C-labeled tetrazine [^{11}C]AE-1 for pretargeted PET imaging

Stéen, E. Johanna L.; Jørgensen, Jesper T.; Petersen, Ida N.; Nørregaard, Kamilla; Lehel, Szabolcs; Shalgunov, Vladimir; Birke, Alexander; Edem, Patricia E.; L'Estrade, Elina T.; Hansen, Hanne D.; Villadsen, Jonas; Erlandsson, Maria; Ohlsson, Tomas; Yazdani, Abdolreza; Valliant, John F.; Kristensen, Jesper L.; Barz, Matthias; Knudsen, Gitte M.; Kjær, Andreas; Herth, Matthias M.

Published in:
Bioorganic and Medicinal Chemistry Letters

DOI:
10.1016/j.bmcl.2019.02.014

Publication date:
2019

Document version
Publisher's PDF, also known as Version of record

Bioorganic & Medicinal Chemistry Letters 29 (2019) 986–990

Contents lists available at ScienceDirect

Bioorganic & Medicinal Chemistry Letters

journal homepage: www.elsevier.com/locate/bmcl

Improved radiosynthesis and preliminary in vivo evaluation of the ^{11}C-labeled tetrazine [^{11}C]AE-1 for pretargeted PET imaging

E. Johanna L. Stéen[a,b,h], Jesper T. Jørgensen[b,c,h], Ida N. Petersen[b,c], Kamilla Nørregaard[b,c], Szabolcs Lehel[b], Vladimir Shalgunov[a], Alexander Birke[d], Patricia E. Edem[a,b,c], Elina T. L'Estrade[a,b,e,f], Hanne D. Hansen[e], Jonas Villadsen[e], Maria Erlandsson[f], Tomas Ohlsson[f], Abdolreza Yazdani[g], John F. Valliant[g], Jesper L. Kristensen[a], Matthias Barz[d], Gitte M. Knudsen[e], Andreas Kjær[b,c,*], Matthias M. Herth[a,b,*]

[a] Department for Drug Design and Pharmacology, Faculty of Health and Medical Sciences, University of Copenhagen, Universitetsparken 2, 2100 Copenhagen, Denmark
[b] Department of Clinical Physiology, Nuclear Medicine and PET, University Hospital Copenhagen, Rigshospitalet, Blegdamsvej 9, 2100 Copenhagen, Denmark
[c] Cluster for Molecular Imaging, Department of Biomedical Sciences, University of Copenhagen, Blegdamsvej 3, 2200 Copenhagen, Denmark
[d] Institute of Organic Chemistry, Johannes-Gutenberg University, Duesbergweg 10-14, D-55099 Mainz, Germany
[e] Neurobiology Research Unit, Rigshospitalet and University of Copenhagen, Blegdamsvej 9, 2100 Copenhagen, Denmark
[f] Radiation Physics, Nuclear Medicine Physics Unit, Skånes University Hospital, Barngatan 3, 222 42 Lund, Sweden
[g] Department of Chemistry and Chemical Biology, McMaster University, 1280 Main Street West, Hamilton, Ontario L8S 4M1, Canada

ARTICLE INFO

Keywords:
PET imaging
Pretargeting
Carbon-11
Tetrazine
Trans-cyclooctene

ABSTRACT

Pretargeted nuclear imaging based on the ligation between tetrazines and nano-sized targeting agents functionalized with *trans*-cyclooctene (TCO) has recently been shown to improve both imaging contrast and dosimetry in nuclear imaging of nanomedicines. Herein, we describe the improved radiosynthesis of a ^{11}C-labeled tetrazine ([^{11}C]AE-1) and its preliminary evaluation in both mice and pigs. Pretargeted imaging in mice was carried out using both a new TCO-functionalized polyglutamic acid and a previously reported TCO-functionalized bisphosphonate system as targeting agents. Unfortunately, pretargeted imaging was not successful using these targeting agents in pair with [^{11}C]AE-1. However, brain imaging in pig indicated that the tracer crossed the blood-brain-barrier. Hence, we suggest that this tetrazine scaffold could be used as a starting point for the development of pretargeted brain imaging, which has so far been a challenging task.

Positron emission tomography (PET) is a routinely used non-invasive and quantitative nuclear imaging technology that allows for biodistribution and pharmacokinetic studies of radiolabeled compounds.[1,2] Apart from this, PET is extremely useful in personalized medicine, where it can provide guidance to identify which patients are likely responders or non-responders to a particular therapy.[3,4] Nanomedicines, such as monoclonal antibodies (mAb), polymers or inorganic nanoparticles have been used successfully as disease-targeting vectors with selective uptake and retention at pathological sites.[5] Unfortunately, very often considerable variations in uptake between patients have been observed and therefore overall treatment outcome would benefit from a pre-screening method capable of selecting responding patients.[5–7] For instance, in 2017 Lee and colleagues used PET imaging to show that the treatment response of human epidermal growth factor 2 (HER2)-targeted liposomal doxorubicin (MM-302) correlated positively with the extent of EPR-mediated uptake of ^{64}Cu-MM-302.[8] This study and similar ones have shown the value of PET-based patient selection in clinical trials to tailor treatment.[8–10]

Conventional nuclear imaging of nanomedicines typically requires long-lived radionuclides, e.g. zirconium-89 ($t_{1/2}$ = 3.3 days), in order to be compatible with their slow target accumulation and clearance.[3] However, since the 1980s, conventional nuclear imaging has been challenged by pretargeted imaging strategies.[11,12] With this approach, the target accumulation and clearance phase of the nanomedicine is separated from the imaging phase, as two distinct agents are used for each phase, as illustrated in Fig. 1. First, a nanomedicine functionalized with a reactive tag (primary targeting agent) is administered and allowed to reach the target tissue. The accumulation of the primary

* Corresponding authors at: Department of Clinical Physiology, Nuclear Medicine and PET, University Hospital Copenhagen, Rigshospitalet, Blegdamsvej 9, 2100 Copenhagen, Denmark.
E-mail addresses: akjaer@sund.ku.dk (A. Kjær), matthias.herth@sund.ku.dk (M.M. Herth).
[h] Equally contributing authors.

https://doi.org/10.1016/j.bmcl.2019.02.014
Received 6 November 2018; Received in revised form 31 January 2019; Accepted 10 February 2019
Available online 13 February 2019

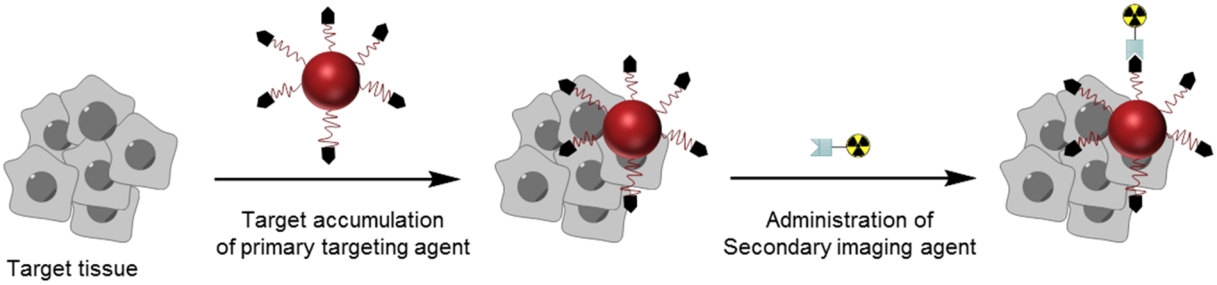

Fig. 1. Schematic illustration of a pretargeting strategy for nuclear imaging. A primary targeting agent functionalized with reactive tags is first administered and allowed to accumulate in the target tissue. In the second phase, the secondary imaging agent is administered. The latter will bind/interact with the compatible reactive tags of the primary targeting agent, which allows for imaging of the targeting agent accumulated in the target tissue.

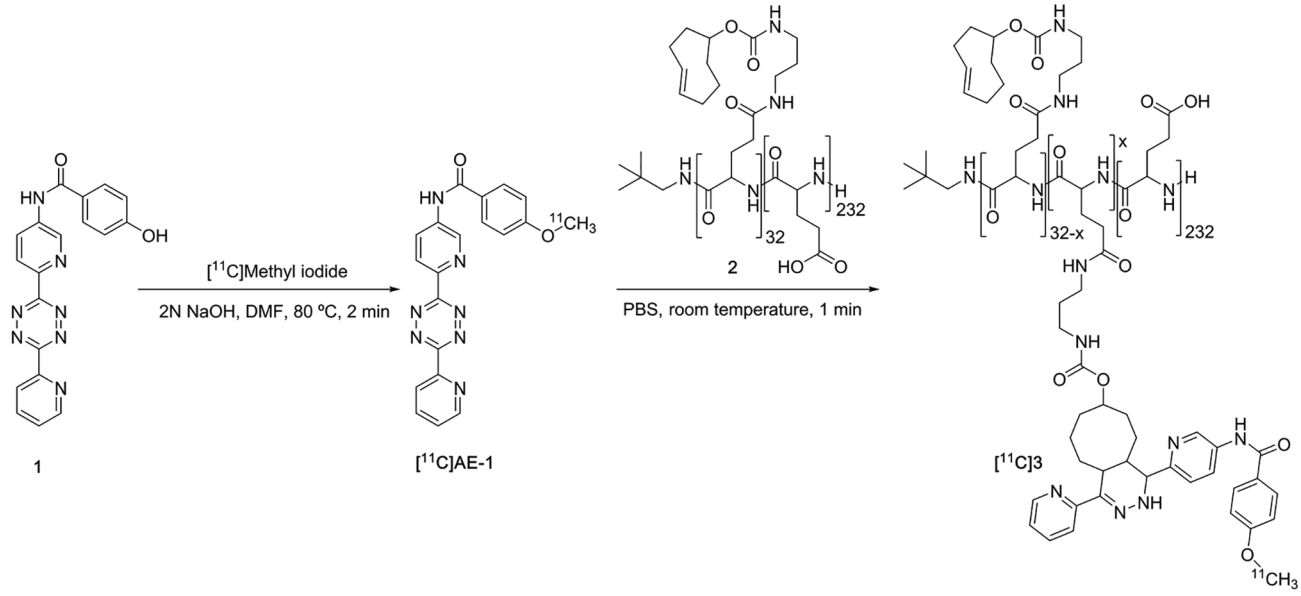

Scheme 1. Radiosynthesis of [^{11}C]AE-1 and subsequent conjugation to TCO-functionalized polyglutamic acid **2**.

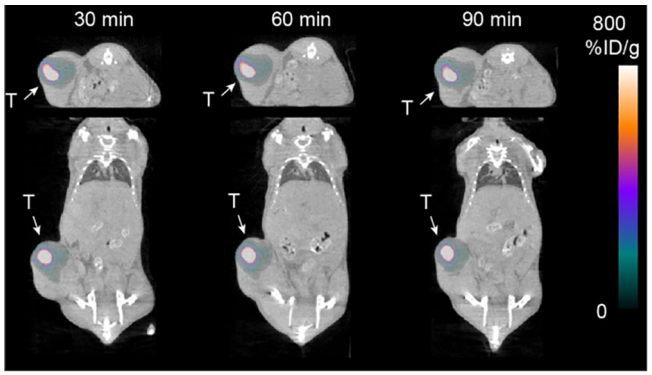

Fig. 2. Representative PET/CT images of mice injected i.t. with [^{11}C]**3** at 30, 60 and 90 min p.i. *Abbreviations:* T = tumor. % ID/g = percentage injected dose per gram of tissue.

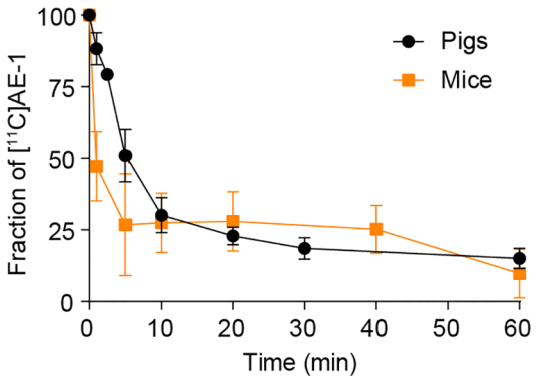

Fig. 3. Stability studies in mice (left, n = 3 per time point) and pig (right, n = 2 per time point). Data are shown as mean and standard error of mean.

targeting agent usually takes several days. After a sufficient period of time, a radiolabeled small molecule (secondary imaging agent) with a compatible reactive tag is administered. The imaging agent will bind selectively to the reactive tag of the nanomedicine, while the excess will rapidly clear from the blood pool. In this way, the nanomedicine is radiolabeled in vivo and the target imaged in a two-step approach. As a result, good imaging contrast can be reached within a short time-frame after injection of the radiolabeled compound, which is not possible for conventional imaging using slow-accumulating nanomedicines. Moreover, the pretargeted imaging strategy enables the use of short-lived radionuclides, thus lowering the radiation burden to the patient.

Modern pretargeting strategies rely on bioorthogonal reactions, i.e. chemical reactions that can proceed in vivo without interfering or interacting with biochemical processes.[13] Besides being inert towards biological moieties, these types of reactions have to be fast. Based on pretargeting strategies used in the clinic, reaction kinetics required for a reaction to be successful in vivo should be within the range of $10^{3-7}\,M^{-1}\,s^{-1}$.[3] Early developed bioorthogonal reactions e.g. the Staudinger ligation, the traceless Staudinger ligation, and the strain-

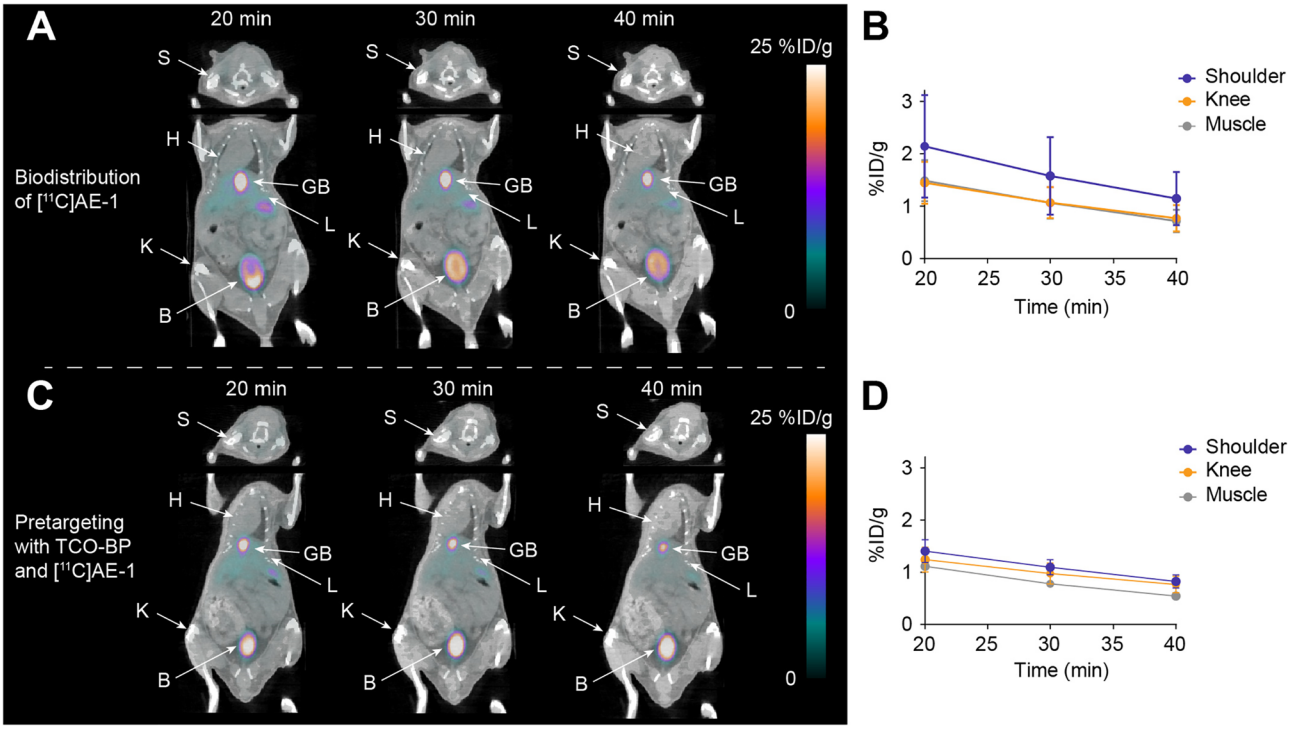

Fig. 4. Pretargeting studies with [^{11}C]AE-1 and TCO-BP. (A) Representative PET/CT images showing the biodistribution of [^{11}C]AE-1 in mice (n = 3) (not pretreated with TCO-BP) at 20, 30 and 40 min p.i. The images show high uptake in the gall bladder and bladder, but no uptake in the shoulders and knees. (B) Extracted uptake values of [^{11}C]AE-1 in shoulder (purple), knee (orange) and muscle (grey) over time, where muscle is expected to have a low-uptake. (C) Representative PET/CT images from pretargeting experiments showing the biodistribution of [^{11}C]AE-1 20, 30 and 40 min p.i in mice pretreated with TCO-BP 1 h prior to tracer administration (n = 3). (D) Extracted uptake values for [^{11}C]AE-1 in shoulder (purple), knee (orange) and muscle (grey) in pretargeting experiments with TCO-BP over time, where muscle is expected to be a low-uptake tissue. *Abbreviations:* S = shoulder; H = heart; GB = gallbladder; L = liver; K = knee; B = bladder.

promoted azide-alkyne [3 + 2] cycloaddition (SPAAC) have seen limited applications in vivo due to their relatively slow reaction kinetics.[13–16] To date, one of the most promising bioorthogonal reactions for pretargeting strategies is the tetrazine ligation, between a 1,2,4,5-tetrazine (Tz) and dienophiles, most frequently *trans*-cyclooctene (TCO).[17] Rate constants up to $10^6\ M^{-1}\ s^{-1}$ have been reported for this ligation.[18] In comparison to the SPAAC, the tetrazine ligation is faster by a factor of approximately $10^{5–8}$ for the most reactive Tz/TCO pairs.[3] A number of successful pretargeted imaging approaches based on the tetrazine ligation have been reported, in which the primary targeting vector is functionalized with TCO-moieties and the Tz is radiolabeled and used as the secondary imaging agent.[19–25] So far, most of the reported Tz-derivatives have been functionalized with different chelators and labeled with radiometals.[19,21,22,26] This restricts pretargeted imaging to extracellular targets since chelators greatly minimize cell membrane permeability. For intracellular targets, either ^{11}C- or ^{18}F-labeled Tz-derivatives would be advantageous. In 2017, Keinänen et al. evaluated a ^{18}F-labeled Tz in pretargeted imaging using internalizing TCO-modified mAbs.[27] This hydrophilic Tz, which was functionalized with a sugar moiety, showed limited use for this specific purpose due to poor cell permeability.[27] Another ^{18}F-labeleld Tz reported by Denk et al. in 2014 has so far not been evaluated in pretargeting studies in vivo.[28] Thus, considerable efforts are directed toward developing ^{11}C- or ^{18}F-labeled Tz-derivatives.[3] Our groups have developed a ^{11}C-labeled Tz, [^{11}C]AE-1 (Scheme 1), which was designed to hold suitable characteristics for pretargeting strategies across cell membranes.[29] Herein, we describe the preliminary in vivo evaluation of [^{11}C]AE-1 in order to validate its utility in pretargeted PET imaging.

The radiosynthesis of [^{11}C]AE-1 (Scheme 1) was carried out as previously reported, i.e. *O*-methylation of precursor **1** using [^{11}C]methyl iodide, but with a few modifications.[29] The formation of a by-product (Supplementary material) was sometimes observed during the semi-preparative high-performance liquid chromatography (HPLC) purification and/or the solid-phase extraction step. The byproduct formation was suggested to arise as a result of radiolysis. This was reduced by changing the HPLC eluent from an acetonitrile (MeCN)-based to an ethanol (EtOH)-based one.[30,31] With the EtOH-based eluent, a radiochemical purity of > 97% could be reached. Isolated radioactivity amounts were 100–250 MBq using a 40 min proton beam (16 MeV beam in a 25 mikroA Scanditronix MC32NI cyclotron) and molar activities (A_m) were in the range of 50–350 GBq/μmol.

In a next step, we investigated the ability of [^{11}C]AE-1 to be used in a tetrazine ligation and therefore tried to ligate it to a TCO-functionalized polyglutamic acid (**2**) (Scheme 1). Polyglutamic acid is an interesting polymer for drug delivery purposes and it is used in several clinical trials.[32] As such, it would be beneficial to use this polymer for personalized medicine approaches. In respect to pretargeted imaging, polymers often display the possibility for higher TCO-loadings compared to mAbs.[3] In light of this, we considered **2** to be an interesting primary targeting vector to evaluate. Synthesis of the polyglutamic acid backbone (p(Glu(COOH)$_{264}$)) was carried out according to Birke et al.[33,34] (synthesis is described in the Supplementary material) and modified with (*E*)-cyclooct-4-en-1-yl(3-aminopropyl)carbamate via amide coupling analogous to a previously reported method.[35] The TCO-conjugate, p(Glu(COOH)$_{232}$-*ran*-Glu(TCO)$_{32}$ (**2**) was characterized via ^{1}H NMR, displaying a TCO-content of 12%, or more specifically 32 TCO-moieties per p(Glu(COOH)$_{232}$) (Figs. S5 and S6). Following the ligation between **2** (0.5 mg in 1 mL phosphate buffered saline (PBS)) and [^{11}C]AE-1, full consumption of [^{11}C]AE-1 was observed after only 1 min at room temperature. The ^{11}C-labeled polymeric ligation adduct [^{11}C]**3** (~7 MBq, apparent specific activity 486 MBq/mg) was injected intratumorally (i.t.) into BALB/c mice bearing CT26 tumors (n = 3). PET/CT images (Fig. 2) up to 90 min post injection (p.i.) displayed no diffusion of [^{11}C]**3** out of the tumor during this time frame.

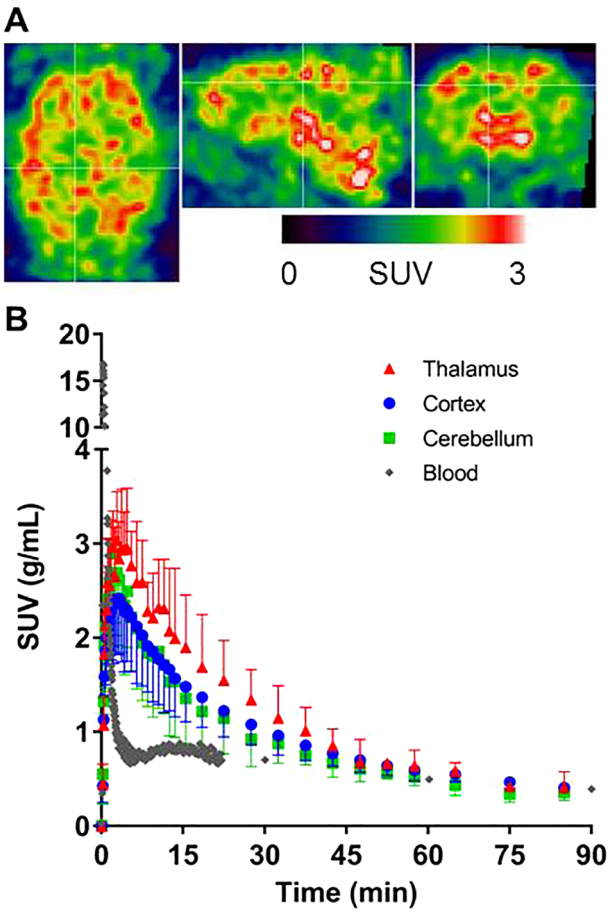

Fig. 5. PET imaging of [^{11}C]AE-1 in pigs (n = 2). (A) Representative transversal (left), sagittal (middle) and coronal (right) PET images (summed images 6–20 min) showing the distribution of [^{11}C]AE-1in the brain of a pig. (B) Regional time-activity curves of [^{11}C]AE-1 in thalamus (red), striatum (purple), cortex (blue) and cerebellum (green) with overlay of distribution in blood (grey). *Abbreviations:* SUV = standardized uptake value (g/mL).

Encouraged by these results, we set up a simplified pretargeting experiment, in which the targeting vector, i.e. polymer **2** (0.5 mg in 50 µL PBS/mouse, n = 2), was injected directly into the tumor, followed by intravenous (i.v.) administration of [^{11}C]AE-1 (~8 MBq, A_m = 190 GBq/µmol). By injecting the targeting vector (**2**) i.t., we aimed to ensure that there was polymer available at the tumor-site to bind the Tz. Moreover, since the data in Fig. 2 showed neglectable polymer diffusion from the tumor for at least 90 min, a 1 h lag time between administration of **2** and [^{11}C]AE-1 for the simplified pretargeting experiments seemed appropriate. Unfortunately, quantification of the PET data showed that there was no specific tumor uptake and high levels of radioactivity were observed in the liver and bladder, as early as 10 min p.i. (Fig. S7A and B). In fact, the biodistribution profile was comparable to the one of [^{11}C]AE-1 in mice not pretreated with **2** (Fig. S7C and D). A possible reason for this could be the in vivo stability of the Tz. As [^{11}C]AE-1 is a highly reactive Tz (the bis-pyridyl substituents makes the Tz framework electron-deficient and extremely reactive toward dienophiles), it is expected to be fairly unstable in vivo.[3] Although the Tz was relatively stable in saline over time (Fig. S8), stability studies in mice (Fig. 3) revealed a rapid degradation of [^{11}C]AE-1 with approximately 47% intact tracer after 1 min. Additional stability studies by radio-TLC (Fig. S16) indicated that the Tz was unstable in plasma and only a small fraction was able to participate in ligation to the TCO-moieties of **2**.

In order to evaluate if the negative results could be attributed to the in vivo properties of **2**, we decided to use an already well-established pretargeting set-up to test the potential of [^{11}C]AE-1 as a secondary imaging agent. In this set-up, a TCO-functionalized bisphosphonate (TCO-BP) was used as a primary targeting vector. The advantage of this set-up is that TCO-BP accumulates fast within sites of active bone metabolism, e.g. knee joints and shoulders, and clears rapidly from the blood pool.[36] As such, pretargeted imaging experiments can be carried out within a single day and without the need of tumor-bearing mice. Consequently, the TCO-BP model is ideal to study pretargeting systems, because of its simplicity and the possibility to accelerate the evaluation process. Pretargeting experiments with TCO-BP were carried out as previously published, but with minor modifications.[36] [^{11}C]AE-1 was applied in tracer doses of high A_m (150–350 GBq/µmol, n = 3) as well as in a carrier added set-up (5 GBq/µmol, 4.2 equivalents of Tz with regard to the molar amount of administered TCOs, n = 3). Additional carrier has been shown to be beneficial in several different pretargeted imaging strategies.[3,27,37] However, there was no difference in the target uptake (shoulder and knee) compared to control experiments (no TCO-BP injected) in neither the high A_m nor carrier-added experiments (Fig. 4). This indicates that the Tz does not react with the TCO-BP in vivo. Alike the pretargeting experiments with **2**, a possible explanation for the unsuccessful experiments is most likely the rapid degradation of [^{11}C]AE-1.

Concurrently, we also evaluated if [^{11}C]AE-1 could be used to image targets across the blood-brain-barrier (BBB). In mice, no significant difference between brain uptake of [^{11}C]AE-1 and blood accumulation (Fig. S7) was found. However, several tracers have shown differences in BBB passage between rodents and higher species, in particular pigs.[38] In light of this, we decided to investigate the BBB penetration of [^{11}C]AE-1 in pigs. Here, [^{11}C]AE-1 showed brain uptake with a high influx rate within the first 5 min (Fig. 5). SUV values of approximately 2.5–3.0 were reached across the brain. As illustrated in Fig. 5B, the activity levels of [^{11}C]AE-1 are higher in brain regions than in blood. This indicated that brain uptake was specific and that the uptake is not solely attributed to radioactivity levels within the brain vasculature. Rapid washout from the brain was observed, which is desirable for a secondary imaging agent for targets within the brain. Long brain retention would only be expected after binding to a TCO-functionalized targeting agent. Stability studies of [^{11}C]AE-1 in pigs showed a slower degradation during the first 10 min compared to in mice, whereafter it was fairly similar (Fig. 3). Overall, more extensive studies have to be performed in order to fully assess the potential of [^{11}C]AE-1 as an imaging agent for targets within the brain. However, at the moment there is no primary targeting agent available for such evaluation studies.

In conclusion, we have herein summarized the results from our preliminary in vivo evaluation of the ^{11}C-labeled Tz, [^{11}C]AE-1. The Tz was successfully applied to radiolabel a TCO-functionalized polyglutamic acid. This ligation adduct was thereafter injected i.t. into tumor-bearing mice, in which no diffusion from the tumor was observed during 2 h of PET/CT scanning. Even though the pretargeting experiments were unsuccessful, the BBB permeability of [^{11}C]AE-1 in pigs is encouraging and [^{11}C]AE-1 could possibly be used to investigate the fate of TCO-functionalized primary targeting agents in the brain. However, further experiments have to be carried out to study the potential to use this Tz for pretargeted imaging across the BBB.

Acknowledgments

The authors wish to thank the H2020 project Click-it under grant agreement no. 668532 for financial support and the technical staff at the Department of Clinical Physiology, Nuclear Medicine & PET at Rigshospitalet. Furthermore, M.B. acknowledges financial support from the CRC 1066-1/2.

Appendix A. Supplementary data

Supplementary data to this article can be found online at https://doi.org/10.1016/j.bmcl.2019.02.014.

References

1. Kristensen JL, Herth MM. *In vivo Imaging in Drug Discovery.* 5th ed. CRC Press; 2017.
2. Herth MM, Knudsen GM. PET imaging of the 5-HT2A receptor system: a tool to study the receptor's in vivo brain function. *Recep Ser.* 2018;32:86–135.
3. Steen EJL, Edem PE, Norregaard K, et al. Pretargeting in nuclear imaging and radionuclide therapy: Improving efficacy of theranostics and nanomedicines. *Biomaterials.* 2018;179:209–245.
4. Theek B, Rizzo LY, Ehling J, Kiessling F, Lammers T. The theranostic path to personalized nanomedicine. *Clin Transl Imaging.* 2014;2(1):66–76.
5. Wicki A, Witzigmann D, Balasubramanian V, Huwyler J. Nanomedicine in cancer therapy: challenges, opportunities, and clinical applications. *J Control Release.* 2015;200:138–157.
6. Harrington KJ, Mohammadtaghi S, Uster PS, et al. Effective targeting of solid tumors in patients with locally advanced cancers by radiolabeled pegylated liposomes. *Clin Cancer Res.* 2001;7(2):243–254.
7. Ramanathan RK, Korn RL, Raghunand N, et al. Correlation between ferumoxytol uptake in tumor lesions by MRI and response to nanoliposomal irinotecan in patients with advanced solid tumors: a pilot study. *Clin Cancer Res.* 2017;23(14):3638–3648.
8. Lee H, Shields AF, Siegel BA, et al. Cu-64-MM-302 positron emission tomography quantifies variability of enhanced permeability and retention of nanoparticles in relation to treatment response in patients with metastatic breast cancer. *Clin Cancer Res.* 2017;23(15):4190–4202.
9. Perez-Medina C, Abdel-Atti D, Tang J, et al. Nanoreporter PET predicts the efficacy of anti-cancer nanotherapy. *Nat Commun.* 2016:7.
10. Dearling JLJ, Packard AB. Molecular imaging in nanomedicine – a developmental tool and a clinical necessity. *J Control Release.* 2017;261:23–30.
11. Reardan DT, Meares CF, Goodwin DA, et al. Antibodies against metal-chelates. *Nature.* 1985;316(6025):265–268.
12. Goodwin DA, Mears CF, Mctigue M, David GS. Monoclonal-antibody hapten radiopharmaceutical delivery. *Nucl Med Commun.* 1986;7(8):569–580.
13. Saxon E, Bertozzi CR. Cell surface engineering by a modified Staudinger reaction. *Science.* 2000;287(5460):2007–2010.
14. Saxon E, Armstrong JI, Bertozzi CR. A "traceless" Staudinger ligation for the chemoselective synthesis of amide bonds. *Org Lett.* 2000;2(14):2141–2143.
15. Nilsson BL, Kiessling LL, Raines RT. Staudinger ligation: a peptide from a thioester and azide. *Org Lett.* 2000;2(13):1939–1941.
16. Agard NJ, Prescher JA, Bertozzi CR. A strain-promoted [3 + 2] azide-alkyne cycloaddition for covalent modification of blomolecules in living systems. *J Am Chem Soc.* 2004;126(46):15046–15047.
17. Blackman ML, Royzen M, Fox JM. Tetrazine ligation: fast bioconjugation based on inverse-electron-demand Diels-Alder reactivity. *J Am Chem Soc.* 2008;130(41):13518–13519.
18. Darko A, Wallace S, Dmitrenko O, et al. Conformationally strained trans-cyclooctene with improved stability and excellent reactivity in tetrazine ligation. *Chem Sci.* 2014;5(10):3770–3776.
19. Rossin R, Verkerk PR, van den Bosch SM, et al. In vivo chemistry for pretargeted tumor imaging in live mice. *Angew Chem Int Ed.* 2010;49(19):3375–3378.
20. Denk C, Svatunek D, Mairinger S, et al. Design, synthesis, and evaluation of a low-molecular-weight (11)C-labeled tetrazine for pretargeted PET imaging applying bioorthogonal in vivo click chemistry. *Bioconjug Chem.* 2016;27(7):1707–1712.
21. Zeglis BM, Sevak KK, Reiner T, et al. A pretargeted PET imaging strategy based on bioorthogonal Diels-Alder click chemistry. *J Nucl Med.* 2013;54(8):1389–1396.
22. Zeglis BM, Brand C, Abdel-Atti D, et al. Optimization of a pretargeted strategy for the PET imaging of colorectal carcinoma via the modulation of radioligand pharmacokinetics. *Mol Pharm.* 2015;12(10):3575–3587.
23. Meyer JP, Houghton JL, Kozlowski P, et al. (18)F-based pretargeted PET imaging based on bioorthogonal Diels-Alder click chemistry. *Bioconjug Chem.* 2016;27(2):298–301.
24. Meyer JP, Kozlowski P, Jackson J, et al. Exploring structural parameters for pretargeting radioligand optimization. *J Med Chem.* 2017;60(19):8201–8217.
25. Albu SA, Al-Karmi SA, Vito A, et al. (125)I-tetrazines and inverse-electron-demand Diels-Alder chemistry: a convenient radioiodination strategy for biomolecule labeling, screening, and biodistribution studies. *Bioconjug Chem.* 2016;27(1):207–216.
26. Evans HL, Nguyen QD, Carroll LS, et al. A bioorthogonal Ga-68-labelling strategy for rapid in vivo imaging. *Chem Commun.* 2014;50(67):9557–9560.
27. Keinanen O, Fung K, Pourat J, et al. Pretargeting of internalizing trastuzumab and cetuximab with a (18)F-tetrazine tracer in xenograft models. *EJNMMI Res.* 2017;7(1):95.
28. Denk C, Svatunek D, Filip T, et al. Development of a F-18-labeled tetrazine with favorable pharmacokinetics for bioorthogonal PET imaging. *Angew Chem Int Ed.* 2014;53(36):9655–9659.
29. Herth MM, Andersen VL, Lehel S, Madsen J, Knudsen GM, Kristensen JL. Development of a (11)C-labeled tetrazine for rapid tetrazine-trans-cyclooctene ligation. *Chem Commun (Camb).* 2013;49(36):3805–3807.
30. Fukumura T, Nakao R, Yamaguchi M, Suzuki K. Stability of C-11-labeled PET radiopharmaceuticals. *Appl Radiat Isotopes.* 2004;61(6):1279–1287.
31. Schuessler H. Effect of ethanol on radiolysis of ribonuclease. *Int J Radiat Biol.* 1975;27(2):171–180.
32. Barz M, Luxenhofer R, Zentel R, Vicent MJ. Overcoming the PEG-addiction: well-defined alternatives to PEG, from structure-property relationships to better defined therapeutics. *Polym Chem.* 2011;2(9):1900–1918.
33. Birke A, Huesmann D, Kelsch A, et al. Polypeptoid-block-polypeptide copolymers: synthesis, characterization, and application of amphiphilic block copolypept(o)ides in drug formulations and miniemulsion techniques. *Biomacromolecules.* 2014;15(2):548–557.
34. Yoo J, Birke A, Kim J, et al. Cooperative catechol-functionalized polypept(o)ide brushes and Ag nanoparticles for combination of protein resistance and antimicrobial activity on metal oxide surfaces. *Biomacromolecules.* 2018;19(5):1602–1613.
35. Barz M, Duro-Castano A, Vicent MJ. A versatile post-polymerization modification method for polyglutamic acid: synthesis of orthogonal reactive polyglutamates and their use in "click chemistry". *Polym Chem-UK.* 2013;4(10):2989–2994.
36. Yazdani A, Bilton H, Vito A, et al. A bone-seeking trans-cyclooctene for pretargeting and bioorthogonal chemistry: a proof of concept study using Tc-99m- and Lu-177-labeled tetrazines. *J Med Chem.* 2016;59(20):9381–9389.
37. van Duijnhoven SMJ, Rossin R, van den Bosch SM, Wheatcroft MP, Hudson PJ, Robillard MS. Diabody pretargeting with click chemistry in vivo. *J. Nucl Med.* 2015;56(9):1422–1428.
38. Syvanen S, Lindhe O, Palner M, et al. Species differences in blood-brain barrier transport of three positron emission tomography radioligands with emphasis on P-glycoprotein transport. *Drug Metab Dispos.* 2009;37(3):635–643.